Folding Properties of Functional Domains of Tropomodulin

Alla S. Kostyukova,*† Elizaveta I. Tiktopulo,† and Yuichiro Maéda*
*Laboratory for Structural Biochemistry, RIKEN Harima Institute at SPring8, 1–1-1 Kouto, Mikazuki-cho, Sayo-gun, Hyogo 679-5148, Japan; and †Institute of Protein Research, Russian Academy of Sciences, Pushchino, Moscow Region 142292, Russia

ABSTRACT Tropomodulin (Tmod) stabilizes the actin-tropomyosin filament by capping the slow-growing end (P-end). The N- and C-terminal halves play distinct roles; the N-terminal half interacts with the N-terminal region of tropomyosin, whereas the C-terminal half interacts with actin. Our previous study (A. Kostyukova, K. Maeda, E. Yamauchi, I. Krieger, and Y. Maéda Y., 2000, *Eur. J. Biochem.* 267:6470–6475) suggested that the two halves are also structurally distinct from each other. We have now studied the folding properties of the two halves, by circular dichroism spectroscopy and by differential scanning calorimetry of the expressed chicken E-type tropomodulin and its large fragments. The results showed that the C-terminal half represents a single, independently folded unit that melts cooperatively through a two-state transition. In contrast, the N-terminal half lacks a definite tertiary structure in solution. The binding of N11, a fragment that corresponds to the first 91 amino acids of the tropomodulin, to tropomyosin substantially stabilized the tropomyosin. This may indicate that the flexible structure of the N-terminal half of tropomodulin in solution is required for binding to tropomyosin and that the N-terminal half acquires its tertiary structure upon binding to tropomyosin.

INTRODUCTION

Tropomodulin is a 40-kDa protein that stabilizes the actin-tropomyosin filament by capping the slow-growing end (P-end). The molecule was originally found as a tropomyosin-binding protein within the spectrin network that lines the erythrocyte membrane (Fowler, 1987) and was later also identified as the P-end capping protein of muscle thin filaments (Weber et al., 1994). Now five isoforms have been identified in a variety of mammalian cell types (Watakabe et al., 1996; Almenar-Queralt et al., 1999; Fischer et al., 2000; Cox and Zoghbi, 2000) as well as in *Drosophila* as the Sanpodo gene product (Dye et al., 1998) and in *Caenorhabditis elegans* (protein sequence accession number T25521).

Tropomodulin inhibits the polymerization and depolymerization of actin monomers at the P-end. This capping is not static and fixed, but dynamic, allowing an exchange of actin monomers with a definite lifetime (Littlefield and Fowler, 1998). Tropomodulin could play important roles in defining actin filament lengths especially in the skeletal muscle sarcomere. This hypothesis is supported by the recent finding that tropomodulin interacts with the N-terminal segments of nebulin (McElhinny et al., 2001), which could be a molecular ruler (Labeit et al., 1991), but it remains to be proved (Littlefield and Fowler, 1998).

Tropomodulin is a bifunctional molecule; the N-terminal half accommodates the interacting site for the N-terminal region of tropomyosin, whereas the C-terminal half is essential for its capping activity, presumably because it contains the actin-binding site (Sung et al., 1992; Sung and Lin, 1994; Gregorio et al., 1995). The nebulin interaction site has not been mapped on tropomodulin.

Substantial progress has been made in our understanding of the functions of tropomodulin (Littlefield and Fowler, 1998). In contrast, the structure of this molecule is only poorly understood. Our knowledge of the structure of tropomodulin, however, will be essential for understanding the molecular mechanism of actin filament pointed end capping. In our previous work, large fragments of tropomodulin were prepared by the use of an improved expression system for recombinant E-tropomodulin, and the fragments were partially characterized. These results indicated that the N-terminal and C-terminal halves of the molecule are distinct from each other, from a structural point of view. Thus, the N-terminal half is highly susceptible to proteolysis whereas the C-terminal half is extremely resistant, suggesting that the N-terminal half is likely to be extended or highly flexible, whereas the C-terminal half is probably compactly folded.

In the present communication, we extended the structural study, especially to determine the folding properties of tropomodulin and its domains. We followed the denaturation process of tropomodulin and its fragments by using circular dichroism (CD) as a probe for the secondary structure and by employing differential scanning calorimetry (DSC) to analyze the tertiary structure. The present results indicated that the two halves of tropomodulin are distinct from each other in their folding properties; the N-terminal half lacks a definite tertiary structure in solution, whereas the C-terminal half represents a single, cooperatively melting domain. Interestingly, the N-terminal half of tropomodulin and the N-terminal end of tropomyosin exhibited drastic structural changes upon binding to each other.

Received for publication 9 February 2001 and in final form 9 April 2001.
Address reprint requests to Dr. Yuichiro Maéda, Laboratory for Structural Biochemistry, RIKEN Harima Institute at SPring-8, 1–1-1 Kouto, Mikazuki, Sayo, Hyogo, Japan 679-5148. Tel.: 81-791-58-2822; Fax: 81-791-2836; E-mail: ymaeda@spring8.or.jp.

0006-3495/01/07/345/07 $2.00

MATERIALS AND METHODS

Protein preparation

Three types of recombinant fragments of chicken E-tropomodulin were prepared. Tmod (N39) (amino acids (a.a.) 1–344) and an N-terminal fragment, N11 (a.a.1–91) were both expressed in *Escherichia coli* with histidine (six residues) tags at the N-termini and were purified according to the method previously described (Kostyukova et al., 2000). A C-terminal fragment, C20 (a.a.160–344), was obtained from Tmod (N39) by proteolysis with *Staphylococcus aureus* V8 protease, as previously described (Kostyukova et al., 2000). Each protein preparation showed a single band on polyacrylamide gel electrophoresis (PAGE) gels (Laemmli, 1970) with and without SDS. The protein concentration was determined by using a Microprotein determination kit (Sigma Chemical Co., St. Louis, MO) with bovine serum albumin as the standard. The isoelectric points were calculated to be 5.2, 5.3, and 6.8 for Tmod (N39), N11, and C20, respectively, by using the ExPASy Proteomics server (Appel et al., 1994), accessible at the internet site of the Swiss Institute of Bioinformatics. To prepare the N11-tropomyosin complex, bovine cardiac tropomyosin was obtained as described previously (Kostyukova et al., 2000). Tropomyosin and the N-terminal tropomodulin fragment N11 were separately dialyzed against 10 mM sodium phosphate, pH 7.6, containing 100 mM NaCl. Three samples, tropomyosin alone, N11 alone, and a mixture of the two, were used for CD and scanning calorimetry measurements. The final concentrations of N11 and the tropomyosin in the samples were 0.9 mg/ml and 0.52 mg/ml, respectively. Degradation of the samples during thermal unfolding was excluded by monitoring them by SDS-PAGE before and after each experiment.

Differential scanning calorimetry

Calorimetric measurements were undertaken with a precision scanning microcalorimeter, SCAL-1 (Scal Co., Pushchino, Russia) (Senin et al., 2000), with glass cells of 0.3-ml volume at a scanning rate of 1.0 K/min. To avoid the aggregation of Tmod (N39) and C20 (see Results), a buffer solution containing no extra salt (25 mM glycine-HCl) was used to adjust the pH between 2.7 and 3.6. Sample preparations in the cells were kept under a constant pressure of 2.0 atm. After the first run of thermal denaturation, the sample was cooled to 3°C and then heated up again to confirm the reversibility. The measured calorimetric trace, the time course of absorbed heat, was corrected for the instrumental baseline, giving rise to the temperature dependence of the partial heat capacity. The analysis of the heat capacity curves was undertaken using equations described previously (Privalov and Khechinashvili, 1974; Privalov and Potekhin, 1986). The real enthalpy of denaturation is determined from the area under the heat capacity peak as

$$\Delta H_{\mathrm{cal}} = MQ_{\mathrm{d}}, \tag{1}$$

where M is the molecular weight and Q_{d} is the excess heat of denaturation referred to 1g of sample. Q_{d} is the area under the peak and above the stepwise function determined by the linear extrapolations of the initial and the final slope of the heat capacity to the middle of the transition (Privalov, 1979). The van't Hoff or the effective enthalpy of the denaturation is obtained as

$$\Delta H^{\mathrm{eff}} = 4RT_d^2\Delta C_{\mathrm{p}}^{\mathrm{max}}/Q_{\mathrm{d}}, \tag{2}$$

where $\Delta C_{\mathrm{p}}^{\mathrm{max}}$ is the height of the heat capacity peak at the midpoint of denaturation (T_{d}). If the heat denaturation is a two-state transition, then the calorimetric enthalpy should be equal to the effective enthalpy:

$$\Delta H_{\mathrm{cal}} = \Delta H^{\mathrm{eff}} \text{ or } \Delta H_{\mathrm{cal}}/\Delta H^{\mathrm{eff}} \approx 1 \tag{3}$$

To obtain parameters such as Q_{d} and $\Delta C_{\mathrm{p}}^{\mathrm{max}}$, the fitting routine based on the two-state transition was employed (Privalov and Potekhin, 1986).

Circular dichroism

The CD measurements were carried out with a spectropolarimeter, model J-725 (Jasco, Tokyo, Japan), with cylindrical fused quartz cells with a path length of 0.1 cm. To avoid the aggregation of Tmod (N39) and C20, the proteins were kept in a solution of low ionic strength, containing 10 mM sodium phosphate, pH 7.6, or 25 mM glycine-HCl, pH 2.7–3.6. From the normalized CD curves, the effective enthalpy was calculated according to

$$\Delta H^{\mathrm{eff}} = 4RT_{\mathrm{d}}^2/\Delta T, \tag{4}$$

where T_{d} is the transition temperature and ΔT is a half-width of the transition. This equation is based upon the assumption that the transition is a two-state process.

RESULTS

In the present study, three types of recombinant fragments of chicken E-type tropomodulin were prepared and used for experiments (Fig. 1). Tmod (N39), consisting of a.a. 1–344 and lacking 15 residues at the C-terminus of the authentic molecule, and the N-terminal fragment N11 (a.a.1–91) were both expressed in *E. coli* with histidine (six residues) tags at the N-termini. A C-terminal fragment, C20 (a.a.160–344), was obtained from Tmod (N39) by proteolysis. The C-terminal 15 residues were removed to avoid heterogeneity in the preparations (Kostyukova et al., 2000). The 15-residue tail may not play an essential role in tropomodulin, because all other isoforms of tropomodulin, except for the E- type, lack at least 15 residues at the C-terminus. For this reason, Tmod (N39) is referred to as the whole molecule in this communication, despite the removal of 15 residues from the C-terminus. All three fragments migrated as single bands when analyzed by a PAGE in the presence of SDS (Fig. 2 *A*) as well as in its absence (Fig. 2 *B*), and showed no aggregation. The mobility of C20 on the native PAGE gel is low because its pI is 6.8, which is close to a neutral pH.

In the beginning, the general stabilities of Tmod (N39) and C20 were studied during urea denaturation and thermal denaturation. At pH 7.6, the thermal denaturation began at 60°C (data not shown) for the two species, as measured by CD at 222 nm, indicating that both are stable polypeptides.

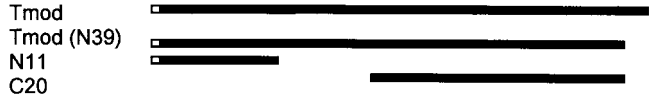

FIGURE 1 The fragments of E-tropomodulin used in the present study. The bars from the top represent E-tropomodulin (Tmod, a.a. 1–359), the N-terminal fragment Tmod (N39) (a.a.1–344, 39.7 kDa), the N-terminal fragment N11 (a.a.1–91, 11.6 kDa), and the C-terminal half C20 (a.a.160–344, 20.6 kDa). The His tags are indicated as open boxes. The amino acid sequence of tropomodulin is numbered from the methionine residue at the original N-terminus.

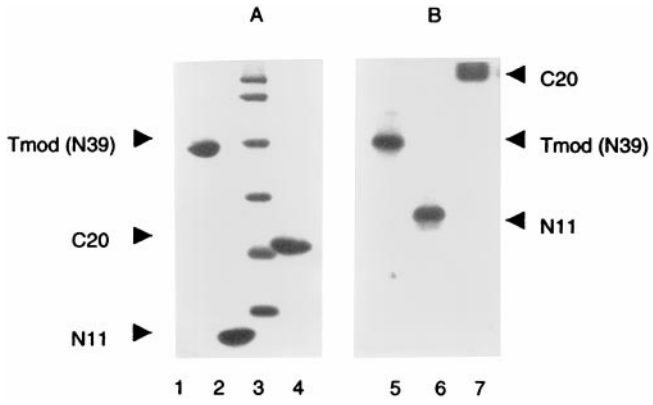

FIGURE 2 PAGE analyses of purified Tmod (N39) and its fragments, on a 15% acrylamide gel in the presence of SDS (*A*) and on a 9% acrylamide gel in the absence of SDS (*B*). Lanes 1 and 5, Tmod (N39); lanes 2 and 6, the N-terminal fragment, N11; lanes 4 and 7, the C-terminal fragment, C20. Lane 3 shows the molecular weight standards of 97,000, 66,000, 42,000, 30,000, 20,100, and 14,400.

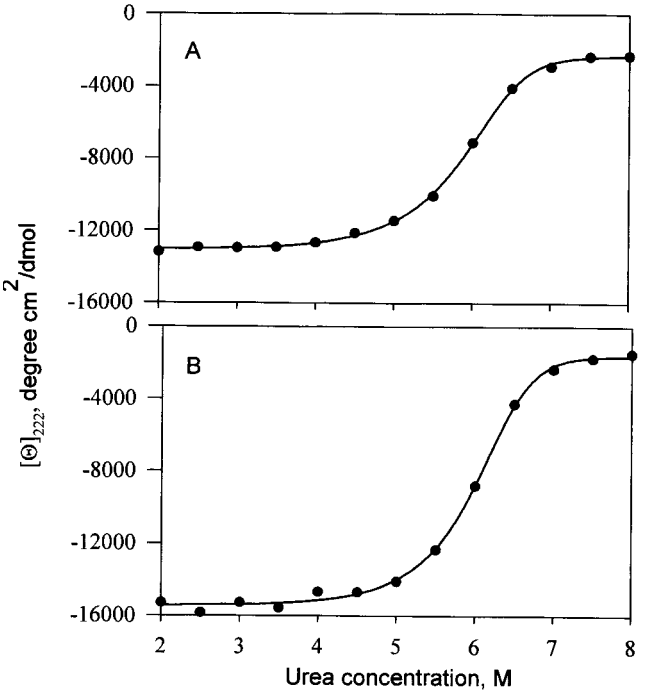

FIGURE 3 Molar ellipticities at 222 nm at various urea concentrations of Tmod (N39) (*A*) and C20 (B) in 10 mM sodium phosphate, pH 7.6.

However, in both species, the heat denaturation was associated with aggregation; Tmod (N39) began aggregating at ~64°C, whereas C20 formed a visible precipitate at 60°C. Both Tmod (N39) and C20 were also stable in the presence of urea. The CD analysis at 222 nm showed that both remained folded in up to 5 M urea, and above that both denatured sharply as the urea concentration increased, with the half-denaturation at 6 M (Fig. 3). The sharp transition to the denatured state is indicative of the cooperative nature of the unfolding process of these two species. In the presence of urea concentrations from 2.5 to 5 M, the thermal denaturation of these proteins was aggregation-free and reversible. The temperature of denaturation, $T_{d,}$ (temperature for half-transition from the native to the denatured state) decreased from 56°C at 2.5 M urea to 42°C at 5 M urea. These results indicated that the unfolding properties of the two proteins are very similar to each other, despite the fact that C20 represents only one-half of Tmod (N39).

To determine how many cooperatively unfolding domains are present within the tropomodulin molecule, DSC measurements were performed. A neutral pH is not suitable for DSC measurements of Tmod (N39) and C20, because of aggregate formation. Although the aggregation problem can be circumvented by adding urea to the solution, this would substantially complicate the thermodynamic parameter calculations, because extrapolation to a zero concentration of urea would be required for all of the data. We found that, at an acidic pH range of 2.6–3.6, the thermal denaturations of Tmod (N39) and C20 were fully reversible and highly cooperative (Fig. 4). With C20, the thermal denaturation was once repeated several times within the glass cell in the DSC apparatus, and the profiles were almost identical to the others, indicating that C20 is extremely stable even under acidic conditions at pH 3. The reversible and cooperative thermal denaturation of the two species at pH 3 was also confirmed by CD at 222 nm. Moreover, the CD spectra of Tmod (N39) and C20 at pH 3 did not essentially differ from those at a neutral pH. Therefore, CD and DSC measurements were undertaken at this pH range. The solution used contained a minimal concentration of pH buffer and no extra salt. The conditions with no salt were required to avoid aggregation and irreversible changes of these proteins (Krieger et al., 2001) and were advantageous for the straightforward deduction of the thermodynamic parameters.

Analyses of the heat capacity peaks showed that the calorimetric and the effective enthalpy coincide well with each other in the cases of both Tmod (N39) and C20. This indicates that the thermal denaturation of the two species is a transition process between two states and that there is only one cooperatively unfolding domain. The thermodynamic parameters obtained from the heat capacity curves are listed in Table 1. The difference between the heat capacities of the native and denatured states is the heat capacity increment, ΔC_p^d, which is used for characterization and comparison of proteins (Fig. 4). The heat capacity increments for Tmod (N39) and C20 are 0.54 and 0.81 cal/g K, respectively (Table 1).

Both the transition temperature and the excess heat of denaturation (Q_d) decreased as the pH decreased (Fig. 5; Table 1). In Fig. 6, the excess heat of denaturation (Q_d) is plotted against the transition temperature, and all of the data points fall on straight lines. The effective enthalpies calculated from the CD temperature curves also fall on these

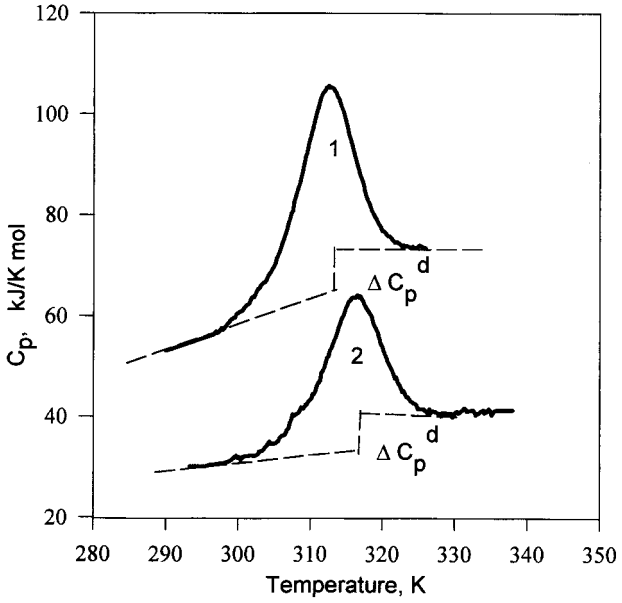

FIGURE 4 Thermal denaturation profiles, the molar heat capacity versus temperature, of Tmod (N39) and C20 measured in 25 mM glycine-HCl, pH 3.0. Curve 1 is for Tmod (N39), and curve 2 is for C20. The heat capacity increment, ΔC_p^d, is obtained as the difference between the heat capacity of the native and denatured states, by extrapolating the initial and the final slope of the heat capacity curves to the transition temperature.

lines, confirming that the melting of the secondary and the tertiary structures occur concomitantly. Extrapolation of the straight lines to 110°C (383 K) gave a Q_d value of ~10 cal/g for C20, which is comparable (if a possible error is taken into account) to the standard value (12–13 cal/g) obtained experimentally for small globular proteins that are tightly folded (Privalov and Khechinashvili, 1974). This value for Tmod (N39) is ~5.5 cal/g, which is about one-half of the value for C20. It is also worth noting that the excess heat of denaturation (Q_d) of the entire molecule is only ~7–11% larger than that of C20, if the magnitudes are compared on a molar basis (Table 1). These results imply that the N-terminal half of the Tmod (N39) molecule is not tightly folded.

This notion that the N-terminal half of tropomodulin is not tightly folded was additionally supported by the experimental results obtained from N11. Our previous CD study showed that N11 has a definite secondary structure (Kostyukova et al., 2000). On the other hand, the CD measurements at 222 nm for N11 indicated that, although its α-helical content decreased with increasing temperature, there was no cooperativity in the melting of this fragment (Fig. 7 *A*). In addition, the DSC measurements on N11 did not reveal a heat absorption peak. These results indicated that although N11 has some secondary structure, it does not form an independent folding unit.

On the other hand, mixing N11 with tropomyosin caused drastic changes in the unfolding properties of tropomyosin, as indicated by the CD (Fig. 7 *A*) and DSC (Fig. 7 *B*) profiles. The heat capacity curves showed that the denaturation of tropomyosin alone occurs as a multi-step process, as previously reported (Potekhin and Privalov, 1982). Upon forming the complex of N11-tropomyosin, major changes occurred in the temperature transition observed at the higher temperature. The transition temperature increased by about 3–4°C, and the excess heat of denaturation increased from 1290 kJ/mol for tropomyosin alone to 1600 kJ/mol for the tropomyosin-N11 complex. This indicates that tropomyosin acquires extra stability upon interacting with N11.

DISCUSSION

The present study clearly indicates that tropomodulin is primarily divided into two parts with distinct folding properties. The N-terminal half has no definite tertiary structure, whereas the C-terminal half forms a tightly folded unit that melts cooperatively through a two-state transition. This conclusion was deduced mainly from two lines of results. First, the stability and folding properties of the folded part of Tmod (N39) and those of C20 are almost identical. Both species are relatively stable and remain folded at temperatures up to 60°C or in the presence of up to 5 M urea (Fig. 3) at neutral pH. Both species aggregate during heat denaturation at neutral pH, whereas both are fairly stable under acidic conditions, pH 2.7–3.6 (Figs. 4 and 5). Both species undergo cooperative denaturation, either by adding urea or by thermal denaturation, and the thermal denaturation occurs through a two-state mechanism. Second, the size of the folding unit within Tmod (N39) is roughly equivalent to that of C20. On one hand, the excess heat of denaturation (Q_d) per mole of the whole molecule is roughly the same as that of C20, with a minimal discrepancy of 7–11%. This difference may not be significant; errors of ~3% may be caused in assaying protein concentrations, and 3–5% errors could also originate from the calorimetric data. The difference of 7–11% might also indicate that cleavage of the N-terminal part from the tropomodulin molecule led to a decrease in the stability of the C-terminal domain. On the other hand, the magnitude of the heat capacity increment for the whole molecule is ~1.3 times larger than that for C20, if the magnitudes are compared on the molar basis (Table 1), although the molecular weight of Tmod (N39) is twice that of C20. The main cause of the heat capacity increment is the hydration of nonpolar groups, which are exposed to the solvent upon disruption of the compact structure of the molecule (Kauzmann, 1959; Sturtevant, 1977). Therefore, the magnitude of the heat capacity increment must be in proportion to the size of the hydrophobic core of a molecule, which includes not only the tightly folded core but also the regions that are denatured without a cooperative transition. In other words, the N-terminal half of the molecule, even without cooperative denaturation, becomes more exposed to the solvent upon heat denaturation. Thus, we conclude that

TABLE 1 Thermodynamic parameters of Tmod (N39) and C20 obtained from differential scanning calorimetry

Sample	pH	C (mg/ml)	T_d (K)	Q_d (cal/g)	ΔH (kJ/mol)	ΔC_p^d (cal/g K)
C20	2.7	0.70	303.4	2.8	242.0	0.081
	3.0	0.70	316.7	4.2	363.0	0.081
	3.3	1.19	323.4	4.65	402.0	0.081
	3.6	0.70	325.5	4.9	423.0	0.081
Tmod (N39)	2.7	0.70	301.6	1.6	266.0	0.054
	3.0	1.40	312.8	2.3	383.0	0.054
	3.3	2.19	323.6	2.6	433.0	0.054
	3.6	1.15	325.5	2.8	466.0	0.054

the N-terminal half of the molecule is not tightly folded and that the major part of the folded core within the whole molecule resides in the C-terminal half, which corresponds to C20. It has been reported that in some other proteins, only a part of the molecule possesses a compactly folded and cooperatively unfolding structure, like ribosomal protein L7 (Gudkov et al., 1978), histones H1, H5, and their fragments (Tiktopulo et al., 1982), and bacterial flagellin (Kostyukova et al., 1988).

The C-terminal half of tropomodulin is a leucine-rich repeat (LRR)-containing domain. This finding resulted from a search for polypeptide sequences homologous to Acan 125, a myosin-I-binding protein that contains a LRR domain (Xu et al., 1997). Later, a homology search of the sequence of C20, using psi-BLAST in combination with visual inspection, also indicated that C20 is a LRR domain (A. G. Murzin, MRC Laboratory of Molecular Biology and Center for Protein Engineering, Cambridge, UK, personal communication). Finally, we have recently obtained the

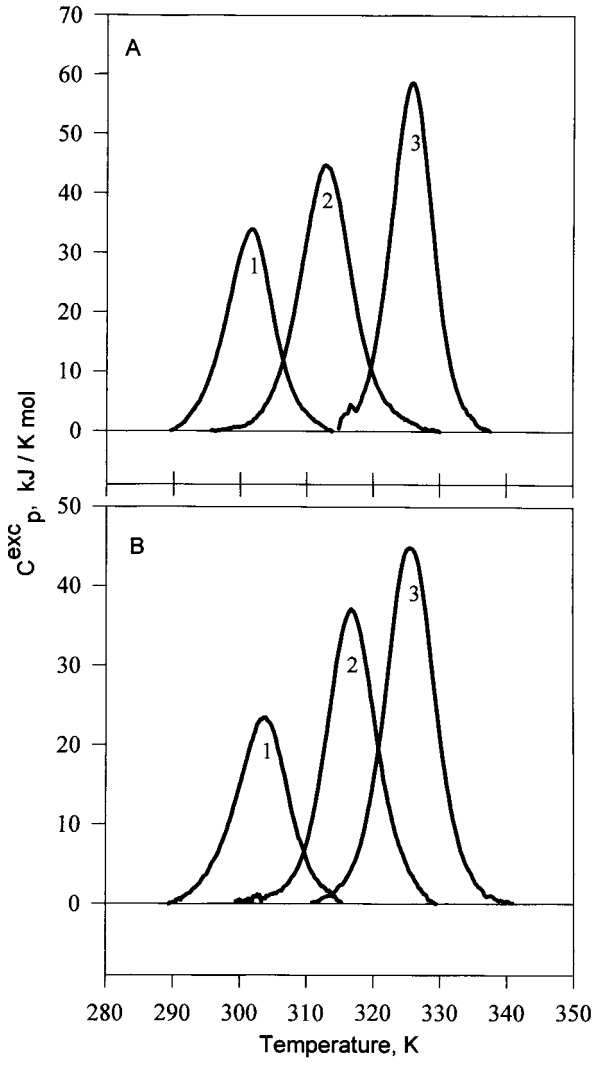

FIGURE 5 Temperature dependence of the excess heat capacity of Tmod (N39) (*A*) and C20 (*B*) measured in 25 mM glycine-HCl at different pH values at pH 2.7 (*curve 1*), at pH 3.0 (*curve 2*), and at pH 3.6 (*curve 3*).

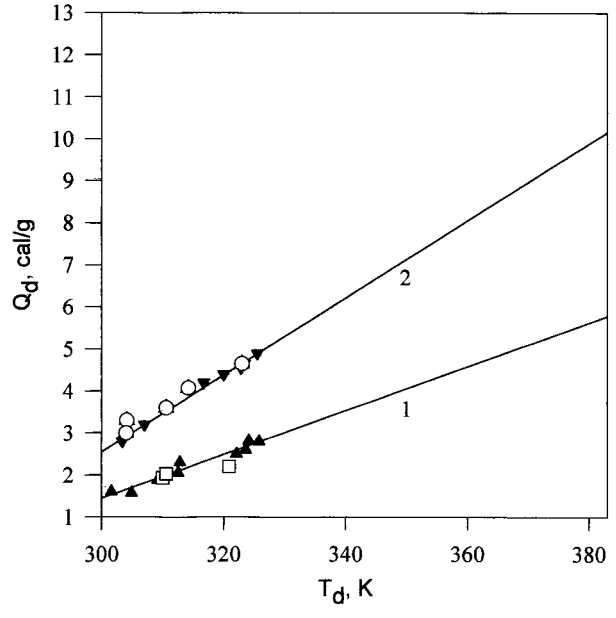

FIGURE 6 Relationship between enthalpy, Q_d, and transition temperature, T_d, for Tmod (N39) and C20. Filled symbols are for Q_d obtained from the heat capacity curves of Tmod (N39) (▲) or of C20 (▼), whereas open symbols are the effective enthalpy calculated by the use of Eq. 4 from the normalized CD curves of Tmod (N39) (□) or of C20 (○). Line 1 is the linear regression line for the calorimetric data points from Tmod (N39), and line 2 is that for C20.

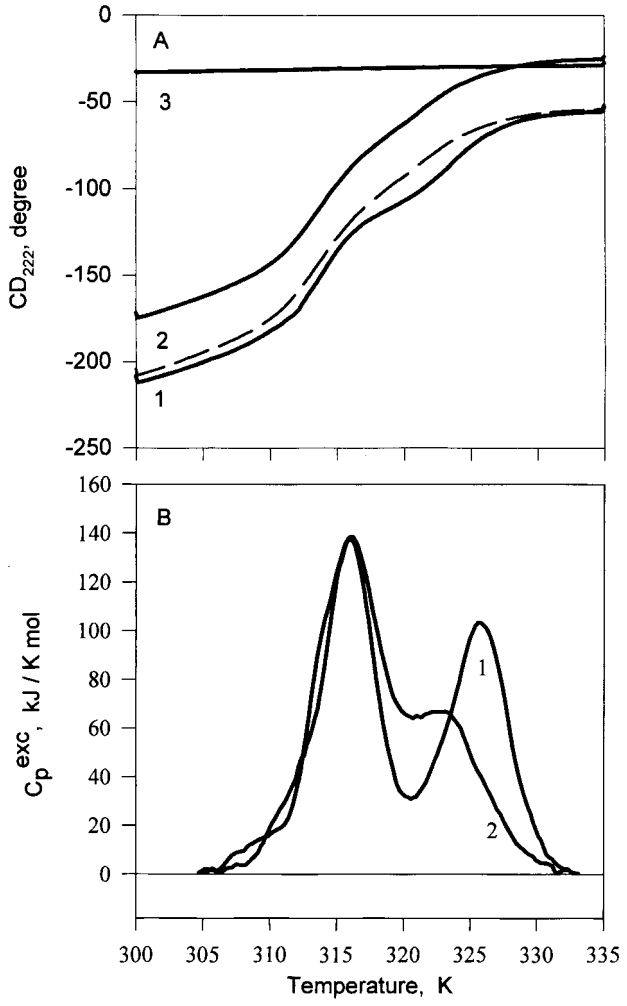

FIGURE 7 Influence of the interaction with N11 on the thermal unfolding of tropomyosin, measured either as the temperature dependence of CD (*A*) at 222 nm or as the temperature dependence of excess heat capacity (*B*). The curves labeled 1 are for the mixture of N11 and tropomyosin with a molar ratio of 10 to 1. The curves labeled 2 are for tropomyosin alone, and curve 3 is for N11 alone. The dashed curve is the sum of the ellipticities of unmixed tropomyosin and N11. The solution condition was 100 mM NaCl, 10 mM sodium phosphate, pH 7.6.

atomic structure of C20 by x-ray crystallography, which unambiguously indicates that C20 consists of a tandem of four to five LRRs, each 28–30 residues long (I. Krieger, A. Kostyukova, A.Yamashita, and Y. Maéda, unpublished results). Therefore, the present study is the first report of the unfolding properties of a LRR protein.

The α-helical content calculated from the CD spectra of Tmod (N39), C20, and N11 were found to be 44%, 46%, and $\sim$ 35% respectively (Kostyukova et al., 2000). This indicates that the α-helical content of the N-terminal half of tropomodulin that interacts with tropomyosin is about the same as that of C20; however, this domain lacks definite tertiary structure. This is based on two lines of results. First, as described above, both the whole molecule and C20 contain a single, cooperatively melting domain of roughly the same size. Second, N11, the N-terminal quarter of the molecule, does not form an independent folding unit (Fig. 7 *A*).

The present results also indicate that tropomyosin becomes more stable upon association with N11; the α-helical content increased (Fig. 7 *A*), and the heat denaturation occurred at a higher temperature and was associated with a larger extent of melting of both the secondary (Fig. 7 *A*) and the (Fig. 7*B*) tertiary structures. The changes in the folding properties of both tropomyosin and N11 may contribute to the extra stability. On the tropomyosin sequence, the tropomodulin interaction site has been mapped to residues 7–14 (Vera et al., 2000). This segment partially overlaps with the first N-terminal 11 residues, which do not form a definite tertiary structure in solution (Potekhin and Privalov, 1982). The site for the interaction with skeletal muscle tropomyosin on the E-tropomodulin polypeptide has been mapped to residues 6–94. Our sequence analysis using MultiCoil (Wolf et al., 1997) indicates that this region has a high propensity for forming a triple coiled-coil. We therefore propose that the binding of tropomodulin to tropomyosin occurs in the following manner. Without an interaction, the N-terminal half of tropomodulin and the extreme N-terminal end of tropomyosin have no definite tertiary structure. The binding of tropomodulin to tropomyosin induces substantial conformational changes in both molecules, so that a triple coiled-coil is formed between the two polypeptide chains of tropomyosin and the one of tropomodulin. The formation of a triple coiled-coil might be associated with the formation of a cooperatively melting domain that stabilizes the complex of tropomyosin and tropomodulin.

As described above, the entire molecule of tropomodulin can primarily be divided into the N-terminal and C-terminal halves. It is worth identifying the minor regions within the two halves. First, there might be a short, flexible tail of 15 amino acids at the extreme C-terminus that is highly susceptible to proteolytic digestion (Kostyukova et al., 2000) and is absent in Tmod (N39). This tail differs in length in the various tropomodulin isoforms (Watakabe et al., 1996; Almenar-Queralt et al., 1999) and may therefore be responsible for isomer-specific functions. Second, there might be a flexible link between the N- and C-terminal halves. The Q_d value (10 g/cal) for C20 obtained by extrapolation is smaller than the standard value (12–13 cal/g) for tightly folded globular proteins. This could be interpreted in terms of an unfolded part within C20, possibly in a region linking the C- and N-terminal halves. The flexible linker could play important roles in the flexible capping of actin-tropomyosin with a tropomodulin molecule consisting of functionally and structurally distinct halves.

Finally, our present view of the conformation of the tropomodulin molecule is substantially different from the previously published models. In one model, at the P-end of actin-tropomyosin, tropomodulin was depicted schematically as a globular protein with a short tail that interacts with

the N-terminus of tropomyosin (Fowler, 1990). In another model, tropomodulin was depicted as a globular protein that has a groove-type binding site for tropomyosin (Vera et al., 2000). In either model, the major part of tropomodulin was thought to form a single globular lobe. Our present study indicates that tropomodulin is divided into two halves that are thermodynamically distinct from each other. Our recent x-ray solution scattering experiments have elucidated the shape and the size of each half, indicating that the C-terminal half forms a globular domain, whereas the N-terminal half is elongated (T. Fujisawa, A. Kostyukova, and Y. Maéda, unpublished results). In summary, we have found that the tropomodulin molecule in solution is divided into two structurally distinct parts; the N-terminal half is elongated in shape and lacks a definite tertiary structure, whereas the C-terminal half is globular in shape and forms an independent folding unit. These properties have prompted us to focus our crystallization efforts upon C20, especially under acidic conditions, where C20 is very stable and does not aggregate (Krieger et al., 2001).

We are grateful to Dr. V. Uversky and Dr. K Vassilenko for advice regarding the CD measurements and to Dr. S. Potekhin for advice about the DSC experiments and his continuous encouragement.

This work was partly supported by the Special Coordination Funds for Promoting Science and Technology of the Ministry of Education, Science and Technology of the Japanese Government.

REFERENCES

Almenar-Queralt, A., A. Lee, C. A. Conley, L. R. de Pouplana, and V. M. Fowler. 1999. Identification of a novel tropomodulin isoform, skeletal tropomodulin, that caps actin filament pointed ends in fast skeletal muscle. *J. Biol. Chem.* 274:28466–28475.

Appel, R. D., A. Bairoch, and D. F. Hochstrasser. 1994. A new generation of information retrieval tools for biologists: the example of the ExPASy WWW server. *Trends Biochem. Sci.* 19:258–260.

Cox, P. R., and H. Y. Zoghbi. 2000. Sequencing, expression analysis, and mapping of three unique human tropomodulin genes and their mouse orthologs. *Genomics.* 63:97–107.

Dye, C. A., J. K. Lee, R. C. Atkinson, R. Brewster, P. L. Han, and H. J. Bellen. 1998. The *Drosophila* sanpodo gene controls sibling cell fate and encodes a tropomodulin homolog, an actin/tropomyosin-associated protein. *Development.* 125:1845–1856.

Fischer, R. S., A. Lee, and V. M. Fowler. 2000. Tropomodulin and tropomyosin mediate lens cell actin cytoskeleton reorganization in vitro. *Invest. Ophthalmol. Vis. Sci.* 41:166–174.

Fowler, V. M. 1987. Identification and purification of a novel Mr 43,000 tropomyosin- binding protein from human erythrocyte membranes. *J. Biol. Chem.* 262:12792–12800.

Fowler, V. M. 1990. Tropomodulin: a cytoskeletal protein that binds to the end of erythrocyte tropomyosin and inhibits tropomyosin binding to actin. *J. Cell. Biol.* 111:471–481.

Gregorio, C. C., A. Weber, M. Bondad, C. R. Pennise, and V. M. Fowler. 1995. Requirement of pointed-end capping by tropomodulin to maintain actin filament length in embryonic chick cardiac myocytes. *Nature.* 377:83–86.

Gudkov, A. T., N. N. Khechinashvili, and V. N. Bushuev. 1978. Studies on the structure of protein L7/L12 from *Escherichia coli* ribosomes. *Eur. J. Biochem.* 90:313–318.

Kauzmann, W. 1959. Some factors in the interpretation of protein denaturation. *Adv. Protein Chem.* 14:1–63.

Kostyukova, A., K. Maeda, E. Yamauchi, I. Krieger, and Y. Maéda. 2000. Domain structure of tropomodulin distinct properties of the N-terminal and C-terminal halves. *Eur. J. Biochem.* 267:6470–6475.

Kostyukova, A. S., M. G. Pyatibratov, V. V. Filimonov, and O. V. Fedorov. 1988. Flagellin parts acquiring a regular structure during polymerization are disposed on the molecule ends. *FEBS Lett.* 241:141–144.

Krieger, I., A. S. Kostyukova, and Y. Maéda. 2001. Crystallization and preliminary characterization of crystals of C-terminal half of tropomodulin. *Acta Crystallogr.* D57:743–744.

Labeit, S., T. Gibson, A. Lakey, K. Leonard, M. Zeviani, P. Knight, J. Wardale, and J. Trinick. 1991. Evidence that nebulin is a protein-ruler in muscle thin filaments [published erratum appears in *FEBS Lett.* 1991, 295:232]. *FEBS Lett.* 282:313–316.

Laemmli, U. K. 1970. Cleavage of structural proteins during the assembly of the head of bacteriophage T4. *Nature.* 227:680–685.

Littlefield, R., and V. M. Fowler. 1998. Defining actin filament length in striated muscle: rulers and caps or dynamic stability? *Annu. Rev. Cell. Dev. Biol.* 14:487–525.

McElhinny, A. S., B. Kolmerer, V. M. Fowler, S. Labeit, and C. C. Gregorio. 2001. The N-terminal end of nebulin interacts with tropomodulin at the pointed ends of the thin filaments. *J. Biol. Chem.* 276:583–592.

Potekhin, S. A., and P. L. Privalov. 1982. Co-operative blocks in tropomyosin. *J Mol. Biol.* 159:519–535.

Privalov, P. L. 1979. Stability of proteins: small globular proteins. *Adv. Protein Chem.* 33:167–241.

Privalov, P. L., and N. N. Khechinashvili. 1974. A thermodynamic approach to the problem of stabilization of globular protein structure: a calorimetric study. *J. Mol. Biol.* 86:665–684.

Privalov, P. L., and S. A. Potekhin. 1986. Scanning microcalorimetry in studying temperature-induced changes in proteins. *Methods Enzymol.* 131:4–51.

Senin, A. A., S. A. Potekhin, E. I. Tiktopulo, and V. V. Filimonov. 2000. Differential scanning microcalorimeter SCAL-1. *J. Therm. Anal. Calorimetry.* 62:153–160.

Sturtevant, J. M. 1977. Heat capacity and entropy changes in processes involving proteins. *Proc. Natl. Acad. Sci. U.S.A.* 74:2236–2240.

Sung, L. A., V. M. Fowler, K. Lambert, M. A. Sussman, D. Karr, and S. Chien. 1992. Molecular cloning and characterization of human fetal liver tropomodulin: a tropomyosin-binding protein. *J. Biol. Chem.* 267: 2616–2621.

Sung, L. A., and J. J. Lin. 1994. Erythrocyte tropomodulin binds to the N-terminus of hTM5, a tropomyosin isoform encoded by the gamma-tropomyosin gene. *Biochem. Biophys. Res. Commun.* 201:627–634.

Tiktopulo, E. I., P. L. Privalov, T. I. Odintsova, T. M. Ermokhina, I. A. Krasheninnikov, F. X. Aviles, P. D. Cary, and C. Crane-Robinson. 1982. The central tryptic fragment of histones H1 and H5 is a fully compacted domain and is the only folded region in the polypeptide chain: a thermodynamic study. *Eur. J. Biochem.* 122:327–331.

Vera, C., A. Sood, K. M. Gao, L. J. Yee, J. J. Lin, and L. A. Sung. 2000. Tropomodulin-binding site mapped to residues 7–14 at the N-terminal heptad repeats of tropomyosin isoform 5. *Arch. Biochem. Biophys.* 378:16–24.

Watakabe, A., R. Kobayashi, and D. M. Helfman. 1996. N-tropomodulin: a novel isoform of tropomodulin identified as the major binding protein to brain tropomyosin. *J Cell Sci.* 109:2299–2310.

Weber, A., C. R. Pennise, G. G. Babcock, and V. M. Fowler. 1994. Tropomodulin caps the pointed ends of actin filaments. *J. Cell Biol.* 127:1627–1635.

Wolf, E., P. S. Kim, and B. Berger. 1997. MultiCoil: a program for predicting two- and three-stranded coiled coils. *Protein Sci.* 6:1179–1189.

Xu, P., K. I. Mitchelhill, B. Kobe, B. E. Kemp, and H. G. Zot. 1997. The myosin-I-binding protein Acan125 binds the SH3 domain and belongs to the superfamily of leucine-rich repeat proteins. *Proc. Natl. Acad. Sci. U.S.A.* 94:3685–3690.